Poster: Scoping Environment to Assist 60 GHz Link Deployment

Sanjib Sur and Xinyu Zhang
sur2@wisc.edu and xyzhang@ece.wisc.edu
University of Wisconsin-Madison

ABSTRACT

Line-of-Sight blockage by human body is a severe challenge to enable robust 60 GHz directional links. Beamsteering is one feasible solution to overcome this problem by electronically steering phased-array beam towards Non-Line-of-Sight. However, effectiveness of beamsteering depends on the link deployment and a lack of assessment of steering effectiveness may render the link completely blacked-out during human blockage. In this poster, we propose a new technique called *BeamScope*, that predicts best possible location for a randomly deployed link in an indoor environment without the need of any explicit war-driving. *BeamScope* first characterizes the environment exploiting measurement from the randomly deployed reference location and then predicts the performance in unobserved locations to suggest a possible redeployment. The environment characterization is captured through a novel metric and prediction is achieved via how this metric is shared between the reference location and unobserved locations. Our preliminary results show promising accuracy of identifying the best possible alternate location for 60 GHz link to achieve a robust connection during human blockage.

Categories and Subject Descriptors

C.2.1 [**Computer-Communication Networks**]: Network Architecture and Design - Wireless communication

Keywords

60 GHz, millimeter-wave, link deployment

1. INTRODUCTION

Millimeter-wave (mmWave) communication is the emerging frontier for next-generation wireless applications. With multi-Gbps data rate, it is a promising technology to support a new plethora of data-hungry applications such as uncompressed video streaming, cordless computing, wireless projector, instant file synchronization and wireless fiber-to-home access. IEEE standard 802.11ad [1] has proposed MAC/PHY design of 60 GHz mmWave frequency band and has already been adopted in few commercial devices *e.g.* Wilocity radio [2]. Figure 1 shows some of the potential indoor application scenarios at 60 GHz.

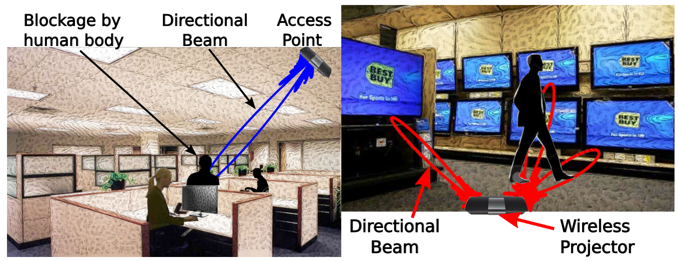

***Figure 1*: Concept applications of 60 GHz.** (a) **Enterprise network.** (b) **Wireless Gbps projector.**

However, 60 GHz links are highly vulnerable to propagation loss. The standard proposal recommends using narrow directional beams formed by phased-array antennas to overcome the strong signal attenuation. But, narrow directional beams at 60 GHz are highly susceptible to human blockages that can occur in indoor deployments with reasonable human activity [3]. A phased-array antenna can electronically steer its beam direction, bouncing the signals off opportunistic reflectors, thus detouring any Line-Of-Sight (LOS) obstacle. However, effectiveness of beamsteering depends highly on the environment *e.g.* availability of any secondary reflective paths *etc.* [4], which depends on the placement of the link.

An obvious way to find out the best possible *spot* to deploy a 60 GHz link would be, to war-drive the entire deployment area covering every *nook and cranny* and deploy the link in best possible *spot*. But two problems pertain to the war-driving, (1) *Overhead*. War-driving is tedious and cumbersome process requiring significant effort from network deployer. Even though an automated robot can be used to scour the place, physical *search space* involving possible combinations of node pair locations can be quite large even for a small $10m \times 10m$ indoor room. (2) *Blockage occurrence*. Exhaustive war-driving may specify best possible *spot* in a human-less indoor room, but it does not consider possible blockage occurrences and their patterns. Rather than using tedious war-driving, in this work we propose an environment scoping algorithm that can find the best *spot* to place 60 GHz link from measurements obtain from a single *spot*.

2. DEPLOYMENT ISSUE OF 60 GHZ LINKS

A LOS 60 GHz link can be extremely susceptible to human blockage if there is no secondary path for the link arrangement. Presence of reflective concrete walls, metallic cabinet *etc.* can provide significant opportunities to bounce the signals off from a secondary path in presence of large obstacles like human body in LOS that

MobiCom'15, September 07–11, 2015, Paris, France
Copyright © 2015 ACM 978-1-4503-3619-2/15/09.
http://dx.doi.org/10.1145/2789168.2795182.

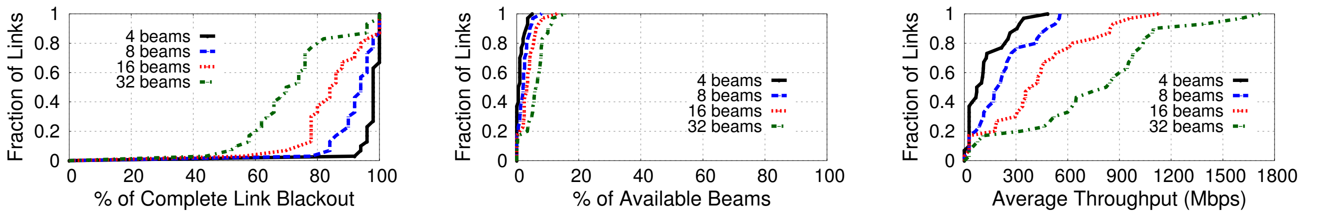

***Figure 2*: (a) Fraction of complete link blackout. (b) Fraction of available beams. (c) Average throughput of best available beam when link is sustained. CDF are plotted across 30 different links during blockage.**

penalizes the link by $20 \sim 30$ dB [3,4]. Figure 2 shows the performance disparity during blockage across 30 different links arbitrary deployed in an indoor office environment. We deploy each link randomly in LOS with 5 m. distance between Tx and Rx. For each link, we emulate random blockage scenarios and collect the performance traces of the phase-array beams during blockage. Figure 2(a) shows the fraction of complete link blackouts during blockage duration (*i.e.* no beam can sustain the connection) and we plot the CDF across the 30 links. For nodes having 32 beams, more than 50% of the links showed atleast 70% of time complete link outage during human blockage. The difference between the fraction of time a complete link outage occurred is significant when comparing a randomly vs. best deployed link [1]. For nodes having 4 beams, this difference is only 8% but grows to 56% when the number of phased-array beams is 32. This shows that a carefully deployed link will be able to sustain the connection during human blockage more effectively than a random one. Further, deployment disparity becomes more severe when the number of phased-array beams increases, which necessitate an environment-aware deployment. Figure 2(b) shows the average number of fraction of available beams during blockage across the 30 different links. Although, we found that as the number of phased-array beams increase, more number of beams are available that can sustain connection, but Figure 2(c) again shows strong disparity between a best link vs. a randomly deployed link. For nodes having 4 beams, the difference of average achievable throughput is only 483 Mbps, while this difference grows to 1.7 Gbps when the number of available beam is 32! This further warrant the requirement of a careful 60 GHz link deployment that can not only sustain the connection more effectively but also may drastically improve link layer throughput during blockage.

3. BEAMSCOPE DESIGN

BeamScope exploits the *sparsity* property of 60 GHz link [5] to establish a *spot* performance prediction framework. The framework *determines the quality of unobserved spot's performance in an environment while observing channel information only from a single measurement spot*. *BeamScope*'s key principle lies in extracting the environmental information from a single measurement *spot* and extrapolating that in an unobserved *spot*. The environmental information is characterized in a novel *environment path skeleton* model during measurement. Furthermore, modeling the way an unobserved *spot* shares the *environment path skeleton* with the measured *spot*, *BeamScope* can predict the performance of it. *BeamScope*'s design can be separated into two different stages: first, when user deploys the link in certain physical positions, *BeamScope* scans the environment by electronically steering pairwise Tx-Rx beams and extracts modeling parameters to construct *environment path skeleton*.

[1]The link that showed best result out of all 30 links, although it may not be an oracle best link.

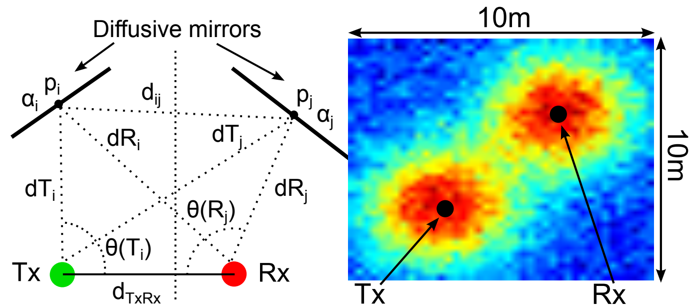

***Figure 3*: (a) Environment as a recursive diffusive mirror. (b) Simulated *BeamScope*'s best beam prediction accuracy in spatial region. Reference Tx and Rx placement is shown. Dark color represents higher accuracy.**

Next, *BeamScope* applies a spatial transfer function over the *environment path skeleton* to infer how the environment should look like from any other *spots* within the environment.

The main idea behind environment scoping from single viewpoint is to extend the aperture of that view-point. *BeamScope* extends the view-point by treating environment as a *recursive diffusive mirror*. The basic idea is simple. When characterizing a part of the environment, use another part of the environment as a diffusive mirror. Figure 3(a) shows an example of characterizing the environment exploiting the recursive mirror concept. Here, while characterizing the object p_i of the environment, we extend the aperture of the receiver Rx by considering object p_j as the diffusive mirror. The receiver Rx's aperture is now extended to fully characterize the object p_i in the environment which includes estimating the distance and the diffusion coefficient. Similarly, while characterizing p_j, p_i is considered as the diffusive mirror.

When the 60 GHz devices are deployed at certain positions, *BeamScope* invokes full beam-scanning procedure (such as in 802.11ad) once to capture the *Channel Impulse Response* (CIR) between each pair of Tx/Rx beams. *BeamScope* then uses matrix $\mathbf{M}$ of $K \times K$ entries to store the CIR of the K received beams from each of the K transmit beam.

When the narrow beam of 60 GHz transmitter incident on an object in the environment, it creates the first signal bounce. This direct bounce is followed by a complex pattern of inter-reflections whose dynamics are governed by the environment geometry and the diffusion property of the material in the environment. At any time instant the receiver observe a projection of the complete set of paths from the environment and this comprises only the paths that are directed towards the receiver and within it receive beam space. Now, lets consider the environment $\mathbb{E}$ comprise of K planar objects $\{p_1, p_2, \ldots, p_K\}$. Let the Euclidean distance vector $\mathbf{dT} = \{dT_1, dT_2, \ldots, dT_K\}$ and $\mathbf{dR} = \{dR_1, dR_2, \ldots, dR_K\}$ denote the distance between the planar object and the transmitter and

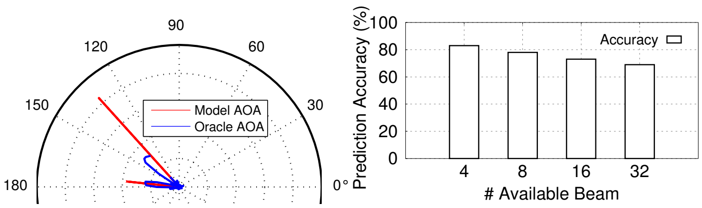

***Figure 4*: (a) Examples of predicting the AOA. (b) *BeamScope*'s best beam prediction accuracy.**

receiver respectively. In addition, let the diffusion coefficient of each planar point is denoted by α_i, which refers to the amount of signal reflected from the point towards direction i. We assume that signals in rest of the directions is uniformly distributed with signal energy is fraction $(1-\alpha_i)$ of the original signal energy. Also, consider $\mathbf{D} = [d_{ij}]$ be the pairwise distance between the planar objects. The *Environment Path Skeleton* is the vector $[\mathbf{dT}, \mathbf{dR}, \alpha]$ comprising of distance of planar object from the transmitter, receiver and the diffusivity. *BeamScope* constructs the *Environment Path Skeleton* using the CIR matrix M. Simply put, each CIR entry m_{ij} in $\mathbf{M}$ contains information about the complete path traversed by the 60 GHz signal which was emitted from a narrow beam at Tx and captured using a narrow beam at Rx. The captured CIR provides with RSS and phase information of signal that interacted and modulated by the environment. To put it concretely, the RSS/phase of the 60 GHz signal transmitted from beam direction T_i and received by beam direction R_j contains information about the distance of Tx from the planar object p_i, the inter-distance between the object p_i and p_j, distance of Rx from p_j and the diffusion coefficient α_i and α_j. Therefore, the amplitude $A(\cdot)$ and phase $\Phi(\cdot)$ of CIR m_{ij} is modeled as,

$$\begin{aligned} A(m_{ij}) &= \frac{\alpha_i \cdot \alpha_j}{dT_i^2 \cdot d_{ij}^2 \cdot dR_j^2} \\ \left(n_{ij} + \frac{\Phi(m_{ij})}{2\pi}\right) \cdot \lambda &= dT_i + d_{ij} + dR_j \end{aligned} \tag{1}$$

In addition, the triangular equality from the Figure 3(a) gives,

$$\begin{aligned} dR_i^2 = &\quad dT_i^2 + d_{TxRx}^2 - 2 \cdot dT_i \cdot d_{TxRx} \cdot cos(\theta(T_i)) \\ dT_j^2 = &\quad dR_j^2 + d_{TxRx}^2 - 2 \cdot dR_j \cdot d_{TxRx} \cdot cos(\theta(R_j)) \end{aligned} \tag{2}$$

We extract the vector $[\mathbf{dT}, \mathbf{dR}, \alpha]$ by jointly solving Equations (1) and (2) for all $i = 1, 2, \ldots, K$ and $j = 1, 2, \ldots, K$.

The *Environment Path Skeleton* captures snapshot of the environment and how a 60 GHz link interacts with it. Therefore, the main step to predict performance in an unobserved *spot* is, to predict how the environment snapshot is supposed to look like from that *spot*. Specifically, we assume that location of the *spot* where we want to predict the performance is known to *BeamScope* system. To simplify the exposition, we assume that we only want to predict unobserved Rx *spot i.e.* Tx is now fixed. Further, the coordinate of the unobserved *spot* is (x_s, y_s) *w.r.t.* the reference coordinate, where the reference coordinate is the position of the Tx. Therefore, predicted *environment path skelenton* from the unobserved *spot* is given by, $[\mathbf{dT}, \mathbf{Tr}_R(\mathbf{dR}), \alpha]$, where $\mathbf{Tr}_R(\cdot)$ denotes the transposition of the distance metric of planar objects from the receiver and calculated using standard coordinate translation method. The translated *Environment Path Skeleton* is converted to the spatial RSS utilizing the Equation (1).

4. EVALUATION

We evaluate feasibility of *BeamScope* by implementing it on a reconfigurable 60 GHz radio platform. We evaluate the feasibility of *BeamScope* of predicting the performance of unobserved from 2 aspects. (1) How accurately *BeamScope* can predict the AOA? (2) What is the accuracy in predicting the performance of best beam?

(1) **Predicting AOA and performance.** We test accuracy of *BeamScope* in predicting the AOA of unobserved *spot* from measurement results obtained from a reference link deployment. We deploy a reference link in an indoor office environment and measure the CIR matrix from Tx-Rx pairwise beamforming. This measurement is used to construct the *Environment Path Skeleton* as per Sec. 3. Further, we move receiver randomly in 8 different *spots*, noted the physical distance from the original receiver *spot* and collect there angular RSS that serve as oracle measurement. The modeled *Environment Path Skeleton* is used to predict the performance in those 8 random *spots* and compared the result *w.r.t.* the oracle measurement. Fig. 4(a) show an example case of predicting the AOA. Further, we compare the prediction accuracy of finding the best beam index in the unobserved *spots* and Fig. 4(b) shows the average accuracy with varying number of available phased-array beams at the receiver side. The accuracy drops as the number of available beams increase.

(2) **Spatial prediction accuracy.** To evaluate the feasibility of *BeamScope* in large-scale, we evaluate the prediction algorithm through simulation. We follow [6] in detail and simulate the interaction of a 60 GHz link in an indoor room (dimension: $10m \times 10m$) with reflective objects deployed randomly. We fixed the reference *spot* of the link and compared the modeled and measured best beam's prediction accuracy. Fig. 3(b) shows the heatmap of the prediction accuracy of finding the best beam in unobserved *spots* using measurement only from the reference link *spot*. This simulation result showcase that the accuracy is poor as we move further away from the reference link. This also suggests the need for collecting measurement from multiple reference *spots* in order to cover the whole indoor area, which we have planned in our future work.

5. CONCLUSION

The poster presents *BeamScope*, a system that scopes the environment to scour best possible location to deploy a 60 GHz link in an indoor environment. *BeamScope* characterizes the environment by capturing sparse path metric. Further, it models the way the metric is shared between unobserved and reference locations and exploits this information to predict the performance in unobserved locations.

6. REFERENCES

[1] IEEE Standards Association, "IEEE Standards 802.11ad-2012: Enhancements for Very High Throughput in the 60 GHz Band," 2012.

[2] "Wilocity 802.11ad Chipset," http://wilocity.com, 2013.

[3] S. Collonge, G. Zaharia, and G. Zein, "Influence of the Human Activity on Wide-Band Characteristics of the 60 GHz Indoor Radio Channel," *IEEE Trans. on Wireless Comm.*, vol. 3, no. 6, 2004.

[4] S. Sur, V. Venkateswaran, X. Zhang, and P. Ramanathan, "60 GHz Indoor Networking through Flexible Beams: A Link-Level Profiling," 2015, proc. of ACM SIGMETRICS.

[5] H. Xu, V. Kukshya, and T. Rappaport, "Spatial and Temporal Characteristics of 60-GHz Indoor Channels," *IEEE Journal on Selected Areas in Communications*, vol. 20, no. 3, 2002.

[6] H. Deng and A. Sayeed, "Mm-Wave MIMO Channel Modeling and User Localization Using Sparse Beamspace Signatures," in *IEEE International Workshop on Signal Processing Advances in Wireless Communications (SPAWC)*, 2014.